

# Outlet design optimization based on large-scale nonsmooth DEM simulation

D. Wang<sup>a</sup>, M. Servin<sup>b</sup>, K-O. Mickelsson<sup>c</sup>

<sup>a</sup>*Umeå University, Umeå, Sweden (da.wang@physics.umu.se).*

<sup>b</sup>*Umeå University, Umeå, Sweden (martin.servin@physics.umu.se).*

<sup>c</sup>*LKAB R&D, Malmberget, Sweden.*

---

## Abstract

We consider the application of a nonsmooth discrete element method to geometric design optimization of a balling drum outlet used in production of iron ore balls. The geometric design optimization problem is based on the need for homogeneous flow of balls from the balling drum onto a wide belt conveyor feeding a roller screen (sieve). An outlet with two design variables is investigated and the optimal shape for the given system and production flow is found by exploring the design space with 2000 simulations.

*Keywords:* Nonsmooth discrete element method, design optimization, mineral processing, balling drum.

---

## 1. Introduction

There is big potential in optimizing particulate flow in mineral and processing technology. Determining the optimal design and control parameters for the systems running on-line in plants is typically too time-consuming, impractical and economically infeasible. This calls for time very efficient simulations that allows exploration of the large design space for the optimization variables.

Simulation based design optimization of systems involving particulate flow is uncommon. Supposedly this is due to that simulations of such systems are associated with long computing times which prohibits systematic approach including exploring large design space. With increasing computing power and advances in the modeling and simulation of granular matter design optimization of complex systems is becoming feasible.

One common method for simulating particulate flow is the *discrete element method* (DEM) [1];[7]. It can be used for simulating granular matter in the gaseous, liquid as well as solid regime whereas many of the alternative methods is best suited for a single regime. In the present paper we use a *nonsmooth DEM* (nDEM) [8] approach, also referred to as the *nonsmooth contact dynamics method* [6];[3]. The particular variant of nonsmooth DEM used in the present paper is described in more detail in an accompanying paper [10]. The nonsmooth approach allows for time integration using time-steps much larger than the characteristic elastic response time and considerable speed-up can be achieved as compared to standard, or *smooth*, DEM. An alternative to DEM would be multiphase computational fluid dynamics [12], e.g., using frictional-kinetic stresses model [11, 9]. However, the width of the gaps in the outlet range down to one particle diameter. At this length scale the continuum models of granular material do not apply.

The current paper considers simulation based geometric design optimization of a balling drum outlet. The purpose is to demonstrate the feasibility of nDEM to this problem and provide a systematic methodology for the geometric design optimization for systems involving particulate flow.

Balling drums are used in agglomeration of powdered mineral ore and binding agency into spherical *green balls* [2]. The balling process precedes the *induration process* where the green balls are hardened into pellets by heating them in a sinter machine. For the sake of quality of the pellets, the ideal goal for the balling process is to produce a nearly *steady flow of spherically symmetric, mono-sized homogeneous green balls* from the balling process. The capacity of the entire pelletizing plant is limited to the maximum flow rate from the balling process that secures high quality pellets. The sieving is maximally efficient when the balls flows over the roller screen in even layer covering the entire screen. This requires that the outlet produce a homogeneous bed of balls. A poor outlet design produces in an inhomogeneous pellet bed and thus less efficient sieving. A homogeneous bed of pellets reaching the end of the horizontal belt conveyor is therefore our basis for formulating the objective function for the design optimization.

We consider a particular balling plant design that is used at LKAB [5] iron ore pelletizing plant MK3 in Malmberget, Sweden. The balling circuits, depicted in Fig. 1 and more schematically in Fig. 2, has the following components: an inclined rotating cylindrical drum with an outlet in the lower end, a wide horizontal belt conveyor where the material lands from the outlet, a roller screen where the material is sieved onto conveyors transporting balls of

correct size (about 10 mm in diameter) further to the sinter machine. Under-sized and over-sized material is conveyed from the sieve, over-sized balls are crushed, and fed back into the higher end of the balling drum together with powdered ore and binding agency. This full scale industrial balling circuit has drum diameter about 3.6 m and circulate material in the range 200-300 tons/hour. A laboratory balling circuit in scale of order 1:4 is under construction in the nearby research facility *Pelletizing Research Centre* (PRC). The design optimization in this paper is for the laboratory balling drum outlet.

## 2. Model of the balling plant

We consider design optimization of a laboratory balling circuit in scale 1:4 scale compared to the one in production. Many parameters of the lab system can be changed. We choose to fix the following geometric parameters: drum diameter  $d \approx 0.75$  m, drum length  $L \approx 2.5$  m, outlet length  $l \approx 0.75$  m, drum inclination  $\theta \approx 7.5$  degrees, conveyor width  $w \approx 1.0$  m and the rotation speed of the drum is  $\omega \approx 2.5$  rad/s. The conveyor velocity is set to  $v = 0.25$  m/s unless otherwise stated. See, Fig. 2, for a simple illustration of the design and notations. The positions of the outlet projected onto the conveyor belt are indicated by the points  $y_1 = 0.15$  m and  $y_2 = 0.9$  m.

The current study is restricted to one particular geometric design of the outlet, illustrated in Fig. 3. It has three gaps with bisector inclination angle  $\eta = 15^\circ$ . The gap width increases with angle  $\alpha$ . The inner base width of the gap at the interface to the drum is denoted by  $\beta$ . These  $\alpha$  and  $\beta$  are our design variables.

The drum, outlet, belt conveyor and roller screen are considered as rigid kinematic objects. The drum and outlet are represented by a mesh of resolution 0.01 m. The drum and outlet is also given a geometric 'texture' consisting of Gaussian shaped bumps randomly distributed with random height in the range [0.002, 0.008] and random width in the range [0.005, 0.02]. The surface density of irregularities is set to 700 dimples per m<sup>2</sup> with random height in the range. The texture has been added to model the presence of agglomerated fine material on the inside of the drum and outlet which causes higher lifting of the balls. The contact force with the rotating drum surface drive the material into a rotational flow in the cross-section plane with an additional flow component in the axial direction by gravity and drum inclination. A close-up from simulation of full scale system is shown in Fig. 4, and an overview is shown in Fig. 5.

The drum is fed with balls at the rate 4.4 kg/s. In the real system the particulate material has a distribution of particle size, mass and moisture content. We model the material as perfectly spherical balls with 10 mm diameter and mass density of 2500 kg/m<sup>3</sup>. The elastic modulus has been measured to be roughly  $Y = 0.5 \times 10^6$  Pa according to Fig. 26 in [2]. The friction coefficient is set to 0.7. From experiments with real balls the coefficient of restitution has been estimated to be close to zero and the friction angle to 35°.

### 3. Simulation

#### 3.1. Nonsmooth DEM

We use nonsmooth DEM for simulating the dynamics of the ore green balls. Each ball is represented as a rigid body. The bodies interact by dry frictional contacts modeled by constraints and complementarity conditions for unilateral nonpenetration and friction according to the Coulomb law. Impacting contacts and stick-slip transitions are considered as instantaneous events making the velocities nonsmooth in time. Our nonsmooth DEM approach, outlined in more detail in Servin et al. [10], allows for time-integration with large time-steps as compared to conventional *smooth* DEM. A particular schema for constraint regularization and stabilization [4] brings both numerical stability and possibility to map the nonsmooth simulation parameters to the conventional viscoelastic material parameters. Time integration  $(x_i, v_i) \rightarrow (x_{i+1}, v_{i+1})$  of the system position  $x$  and velocity  $v$  from time  $t_i$  to  $t_{i+1} = t_i + h$  involve solving a mixed linear complementarity problem (MLCP) of the form

$$\begin{bmatrix} M & -G_i^T \\ G_i & \Sigma \end{bmatrix} \begin{bmatrix} v_{i+1} \\ \lambda_{i+1} \end{bmatrix} = \begin{bmatrix} p_i \\ q_i \end{bmatrix} \quad (1)$$

with friction cone conditions  $\lambda \in \mathcal{C}(\mu\lambda_n)$

$$\mathcal{C}(\mu\lambda_n) \equiv \{\lambda = [\lambda_n, \lambda_{t_1}, \lambda_{t_2}] : \lambda_n \geq 0, |\lambda_t| \leq \mu|\lambda_n|\}$$

on the Lagrange multiplier,  $\lambda$ , for the constraint force,  $G^T \lambda$ , responsible for maintaining non-penetration in the contact normal direction  $n$  and Coulomb dry friction in the contact tangent plane spanned by  $t_1$  and  $t_2$ . The submatrices  $M$  and  $\Sigma$  are block diagonal matrices of body mass and contact regularization, respectively. The submatrix  $G$  is block sparse contact Jacobian built of by normal and tangent vectors. The constraints regularization,

$\Sigma$  and stabilization terms  $q_i$  are based on the energy and dissipation potentials from Hertz contact law and thus link the parameters of the numerical integration scheme directly to measurable or tabulated viscoelastic material parameters. For spheres, the Hertz contact law reads  $f = k(g^{3/2} + cg^{1/2}\dot{g})$ , where  $f$  is the force,  $g$  the contact overlap,  $k$  the stiffness coefficient and  $c$  the damping coefficient. We use constraint regularization and stabilization terms [10] that map to  $k = 25 \text{ kN/m}^{3/2}$  and  $c = 0.02 \text{ s}^{-1}$ . For impacting contacts, we instead apply zero restitution, which corresponds to setting  $q_i = 0$  in Eq. (1). The time-step  $h$  should be a fraction of  $R/v_n$  not to cause too big contact overlaps, where  $v_n$  is the characteristic relative normal velocity in the contact points and  $R$  is the ball radius. In the drum, the material shear rate is roughly  $\dot{\gamma} \approx \Delta v/\Delta x \approx \omega d/h_p$ , where  $h_p \approx 20R$  is the height of the material in the drum and we assume to have a dense flow with velocity scaling linearly from the drum surface to the top surface. The relative contact velocity between two particle layers is thus estimated to  $\dot{\gamma}2R \approx \omega d/10 \approx 0.2 \text{ m/s}$  such that  $R/v_n \approx 0.25 \text{ s}$ . We therefore choose time step  $h = 0.01 \text{ s}$ . The time integration includes solving a mixed linear complementarity problem (MLCP) condition with  $3N_p + (3/2)Nc \sim 6N_p$  variables assuming the  $N_p$  particles has on average 6 contacting neighbours summing to  $N_c$  contacts in total. The simulation involves approximately 80k particles, which means 500k variables. The contact constraint forces and resulting velocity changes are computed using a projected Gauss-Seidel solver for the MLCP. The number of iterations are set to 25.

The computational time for simulation of one drum evolution (2.6s) with 80k particles is measured to be 585s, i.e., average computational speed for 1k particle is 2.8s computing time for 1s real time. The simulation are r-un single threaded and on a desktop computer Intel(R) Core(TM) Xeon X5690 3.46 GHz processor. Sample simulations with full scale drum and up to 1.8M particles, shown in Fig. 4 and Fig. 5, runs on a desktop computer with 16 GB RAM memory.

Video from simulation is available on the web: <http://umit.cs.umu.se/granular/outlet>.

### 3.2. State initialization

An initial state close to stationary flow is produced by running a simulation for 40 s, (approximately 15 drum evolutions) with iron ore balls added in the rate of 4.4 kg/s at the upper end of the drum. Particles reaching the belt

conveyor are deleted during the simulation. This state – consisting of  $N_p$  position vectors, velocity vector and angular momentum vector plus drum and outlet orientation – is used for each simulation in the design optimization. To let the flow adapt to a new outlet geometry each simulation is initialized by another 10.4 s (4 drum evolutions) of simulation before recording starts.

### 3.3. Recording

The position of each particle reaching the belt conveyor is stored together with the time of impact. The particle is then removed from the simulation in order to save computational time. Recording is made during a time-interval of two drum evolutions (5.2 s). The positions and time are transformed into a coordinate system co-moving with the belt conveyor, i.e.,  $(x, y, t) \rightarrow (x - vt, y)$ . A sample recording of particle positions on conveyor from one simulation is shown in Fig. 6. The flow inside the drum was observed to be close to stationary after more than 10 s of initialization, i.e., there was no sign of flow instabilities or pulsating phenomena. The characteristic and expected striped pattern on the conveyor belt contact data is due to the outlet gaps and the time duration of the recording is six times of the gap periodicity.

### 3.4. Surface reconstruction

The particles impacting the belt conveyor forms a bed with some height surface shape  $h(x - vt, y)$  m. We use *cellular automata* [7, Ch. 6] to reconstruct this surface from the particle scatter data. The number of particles on the conveyor data in Fig. 9 is roughly 200 k, compared to roughly 80 k in the drum. Hence, simulating all particles would take 3.5 times longer time. Also, stable pile formation would require adding constraint based rolling resistance, which would add additional  $2 \times N_c$  equations to the MLCP solved at each time-step. The net effect would be an increase in CPU time by more than 5 times. The cellular automata operates on a regular square grid with cell size of 2.5 particle diameters, friction angle  $35^\circ$  (measured in tests) and packing ratio of 0.7. The surface reconstruction of the particle data in Fig. 6 is shown in Fig. 7.

## 4. Design optimization

### 4.1. Objective function

The goal is to determine the values of the design variables  $(\alpha, \beta) \in \mathcal{D}$  for the outlet geometry that produces an even flow of iron ore balls onto the

sinter screen. By even flow we mean that the height of the iron ore ball bed reaching the end of the belt conveyor has constant cross-section when time-averaged over one drum evolution  $t_d = 2\pi/\omega$ . The rotating outlet typically produces stripes of pellets on a the conveyor belt, see Fig. 7. If the stripes are perfectly uniform it is possible to find a velocity of the belt conveyor that compress the stripes into a planar surface. The time averaged pellet bed height is computed:

$$h(t, y) \equiv \frac{1}{t_d} \int_0^{t_d} h(x_0 - v(t + \tau), y) d\tau \quad (2)$$

If the flow of iron ore balls inside the drum is stationary when reaching the outlet the time-averaged height of the iron ore ball bed will be constant in time and we denote it  $h(y)$ . Any discrete height profile  $h(y)$  can be represented by its fast Fourier transform (FFT) with complex amplitudes  $a_n$ ,  $n = 0, \pm 1, \pm 2, \dots, \pm N$ . Each mode contributes to variations of the height profile with magnitude  $|a_n|/N$  and wave length  $l_c/\pi|n|$ , where  $l_c$  is the width of the conveyor. A constant profile would correspond to  $h(y) = a_0/N$  and  $a_n = 0$  for all  $n \neq 0$ . The low mode number variations ( $n \neq 0$ ) are the most negative ones for the sintering performance. Higher modes correspond to short wave length fluctuations that disperse more easily on the sinter screen. Therefore we introduce a decaying weight factor  $w_n = 2^{|n|-1}$  and chose the following objective function

$$f(\alpha, \beta) = \frac{1}{N} \sum_{n=1}^N w_n \left( \|a_{-n}\| + \|a_n\| \right) \quad (3)$$

We use  $N = 20$  modes in the design optimization. The optimal design parameter pair is the solution to  $\arg \min_{(\alpha, \beta) \in \mathcal{D}} f(\alpha, \beta)$ , where the design space  $\mathcal{D}$  is the domain of objective function. Since the object function is based on the time averaged height profile the result depends very weakly on the choice of conveyor speed. The effect on the value of the objective function at the optimum by reducing the speed by half or doubling it was found to be 4%. The conveyor velocity is also limited from below and above to avoid high pellet beds and high impact velocities at the roller screen.

#### 4.2. Optimization procedure

The objective function cannot be assumed convex and local minima might exist. This calls for heuristic strategy in finding optimal solution. In the first

stage a large design space,  $\mathcal{D}_1$ , is chosen. The space is covered by a regular grid of  $\sim 200$  nodes, each corresponding to a simulation with particular value for  $(\alpha, \beta)$ . Potential regions of optimum are investigated further in successive stages. If the objective function appears smooth various local optimization techniques may be applied. We set the procedure is terminated when we found a solution of which all amplitudes  $a_n \leq \frac{1}{10}a_0$  for all  $N \geq 1$ . That suggests the objective function deceeds the chosen tolerance threshold,  $\|f(\alpha, \beta)\| < \epsilon_h = 0.01$  m.

## 5. Results

### 5.1. Optimal design

The first stage analysis of the objective function in the design space start with a series of simulations in region  $\alpha \in [0^\circ, 0.6^\circ]$  and  $\beta \in [0.01, 0.2]$  m with a coarse grid. That give us a first rough view of the objective function in the design space.

At the second stage we zoomed in on the region  $\mathcal{D}_1$  with  $\alpha \in [0.1^\circ, 0.4^\circ]$  and  $\beta \in [0.03, 0.07]$  m. The result from 768 simulations, which cost about one hour each to run, provides us an convex surface with some noise.

The third stage is carried out on a smaller region with higher resolution grid,  $\mathcal{D}_2$  with  $\alpha \in [0.12^\circ, 0.33^\circ]$  and  $\beta \in [0.034, 0.06]$  m contains 864 simulations.

The optimum solution is found  $(\alpha_I, \beta_I) = (0.20^\circ, 0.048$  m) with error tolerance  $(\Delta\alpha, \Delta\beta) = (0.01^\circ, 0.003$  m). We show the contour plot of combined 2nd stage and 3rd stage grids in Fig. 8. Note that the bold line is the border of the chosen tolerance threshold  $\|f(\alpha, \beta)\| < \epsilon_h$ .

### 5.2. Sample data

We provide more detailed simulation results for four sample points listed in table 1. For each data point we present the particle position scatter plots on belt conveyor, post-processed surface, the time-integrated height profile and the corresponding FFT spectrum that builds up the objective function value. These data are found in Fig. 9.

### 5.3. Observations

We make the following observations. A too wide angle and too wide base width results in too big outflow between the gaps and formation of a heap

Table 1: Sample points

Point	$\alpha$ [degree]	$\beta$ [m]	$f(\alpha, \beta)$ [m]	Comment
I	0.20	0.048	0.006	optimum
II	0.17	0.051	0.010	on the tolerance
III	0	0.01	0.077	too narrow gaps
IV	0.6	0.2	0.045	too large gaps

under the edge between the end of the drum and the outlet (data point IV). A too narrow angle and too narrow base width produces too small outflow between the gaps resulting in a heap under the end of the outlet. There is no point in the design space that produces a planar bed of ore balls. The optimal solution (I) has a constant rate of outflow between the gaps along the axial direction ( $y$ -axis) but the outlet is too short for all particles to spread evenly. The 'excessive' particles form a heap at the end of the outlet.

## 6. Discussion

There are a number of uncertainties in the model and simulation that must be remedied before the presented design optimization method have fully known predictive power. These include the choice of material and model parameters (size distribution, friction, geometric shape, etc.) and simulation parameters (time-step, number of iterations). The latter is thoroughly considered in a separate publication [10]. Validation of remaining model parameters, foremostly the contact model of the drum wall, is left for future work when the lab drum system is installed and in operation. The result, that the particular design principle considered in this work cannot produce a planar height profile, is likely to remain. Furthermore, it is improbable that this design principle will be optimal for a range of different input mass flow. Alternative design principles are called for and the presented method can be applied to design exploration and sensitivity analysis and finally optimization of the design.

## 7. Conclusions

Design optimization of balling plant outlet geometry based on nonsmooth DEM simulation has been shown feasible. The relevant design space was

covered by approximately 2000 simulations of 15.6 s material flow each with  $80 \times 10^3$  particles. The total computational time was  $7.6 \times 10^6$  CPU seconds (2100 hours or 88 days). We used a computer with 12 CPUs in which case the total time for the design optimization procedure was roughly seven days of computation. With this performance it is possible to cover alternative designs that requires a larger design space. The conclusion from the design analysis is that the particular outlet design considered has no solution for which a planar bed can be produced. One solution is found that produces a even outflow but the outlet form a heap at the end. Future steps involve sensitivity analysis of model and simulation parameters as well as of the realization of stationary flow. Alternative outlet design will be considered that avoids the formation of a heap at the end.

## 8. Acknowledgements

This project was supported by LKAB, ProcessIT Innovations, UMIT Research Lab and by Algoryx Simulations.

## 9. References

- [1] Cundall, P. A., Strack, O. D. L., 1979. A discrete numerical model for granular assemblies. *Geotechnique* 29, 47–65.
- [2] Forsmo, S., 2007. Influence of green pellet properties on pelletizing of magnetite iron ore. Ph.D. thesis, Luleå University of Technology, Luleå.
- [3] Jean, M., 1999. The non-smooth contact dynamics method. *Computer Methods in Applied Mechanics and Engineering* 177, 235–257.
- [4] Lacoursière, C., 2007. Regularized, stabilized, variational methods for multibodies. In: Peter Bunus, D. F., Führer, C. (Eds.), *The 48th Scandinavian Conference on Simulation and Modeling (SIMS 2007)*, 30-31 October, 2007, Göteborg (Särö), Sweden. Linköping Electronic Conference Proceedings. Linköping University Electronic Press, pp. 40–48.
- [5] LKAB, 2011. URL <http://www.lkab.com>
- [6] Moreau, J. J., 1999. Numerical aspects of the sweeping process. *Computer Methods in Applied Mechanics and Engineering* 177, 329–349.

- [7] Pöschel, T., Schwager, T., 2005. Computational Granular Dynamics, Models and Algorithms. Springer-Verlag.
- [8] Radjai, F., Richefeu, V., 2009. Contact dynamics as a nonsmooth discrete element method. *Mechanics of Materials* 41 (6), 715–728.
- [9] Shuyan, W., Xiang, L., Huilin, L., Long, Y., Dan, S., Yurong, H., Yonglong, D., 2009. Numerical simulations of flow behavior of gas and particles in spouted beds using frictional-kinetic stresses model. *Powder Technology* 196 (10), 184193
- [10] Servin, M., Bodin, K., Lacoursière, C., Wang, D., 2013. Examining the smooth and nonsmooth discrete element approach to granular matter. Accepted for publication in *International Journal for Numerical Methods in Engineering* (2013).  
URL <http://umit.cs.umu.se/granular/dem>
- [11] Srivastava, A., Sundaresan, S., 2003. Analysis of a frictionalkinetic model for gasparticle flow. *Powder Technology* 129 (1), 72-85.
- [12] van Wachem, B. G. M., Almstedt, A. E., 2003. Methods for multiphase computational fluid dynamics. *Chemical Engineering Journal*, 96 (13), 81-98.

12



Fig. 1: A balling plant showing part of the balling drum, outlet, belt conveyor and roller screen. Picture courtesy of LKAB.

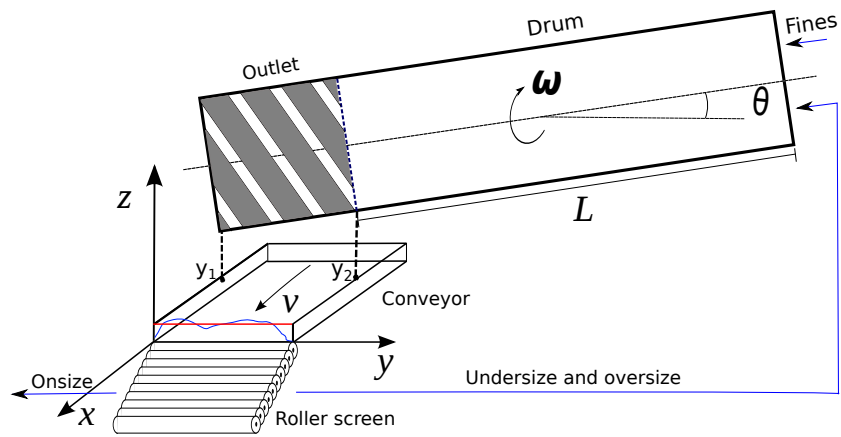


Fig. 2: Drum configuration.

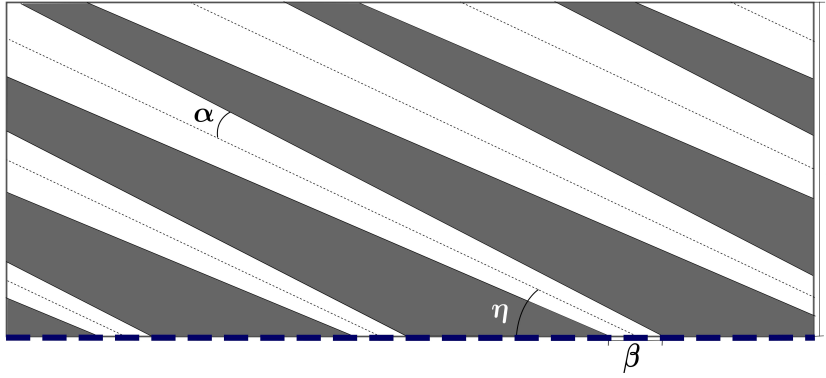


Fig. 3: 2D-projection of the outlet clarifying the design parameters angle and width.



Fig. 4: Capture from simulation showing material flow from the outlet onto the conveyor and roller screen.

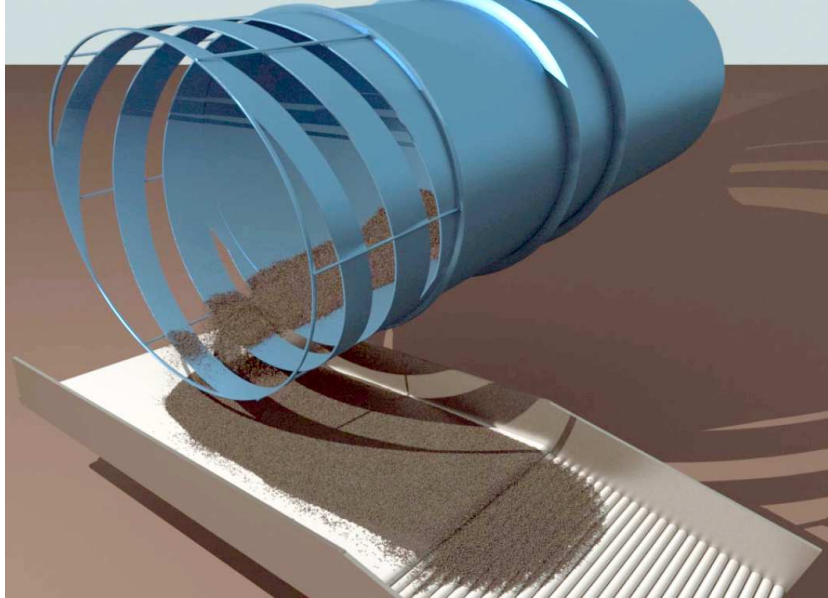


Fig. 5: Capture from simulation showing overview of the balling plant.

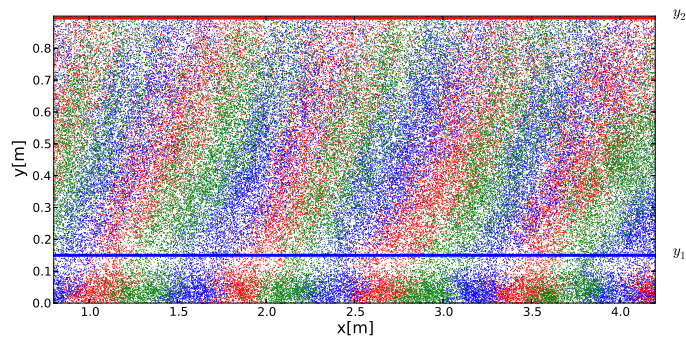


Fig. 6: The particles hitting the conveyor is stored as point scatter in a 2D surface. Particles are colored in red, blue or green depending of which of the three gaps it exited. The projected position of the outlet is at  $y_1$  and  $y_2$ .

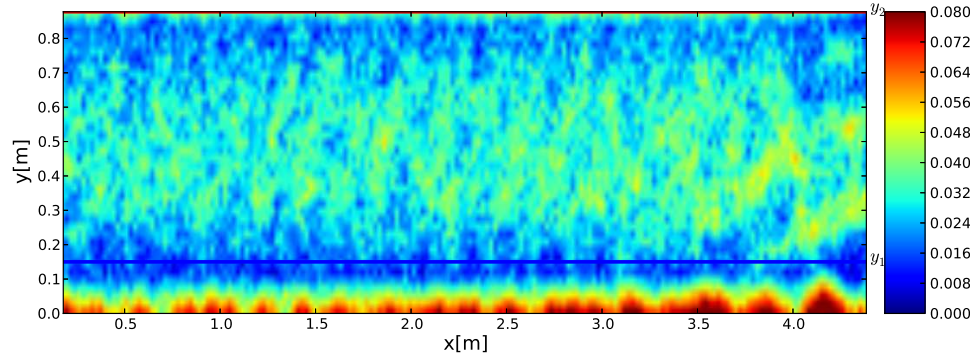


Fig. 7: Particle 2D height surface on conveyor reconstructed from particle impacts. The color codes the height in units m. The projected position of the outlet is at  $y_1$  and  $y_2$ .

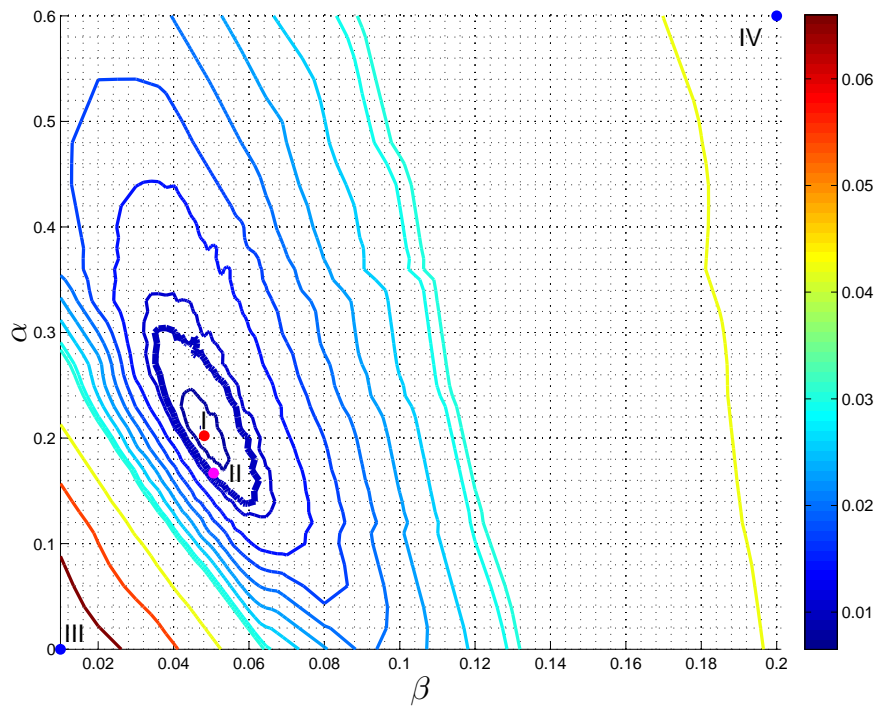


Fig. 8: Contour plot of objective function  $f(\alpha, \beta)$  from simulations. The color codes the value of the objective function in unit m.

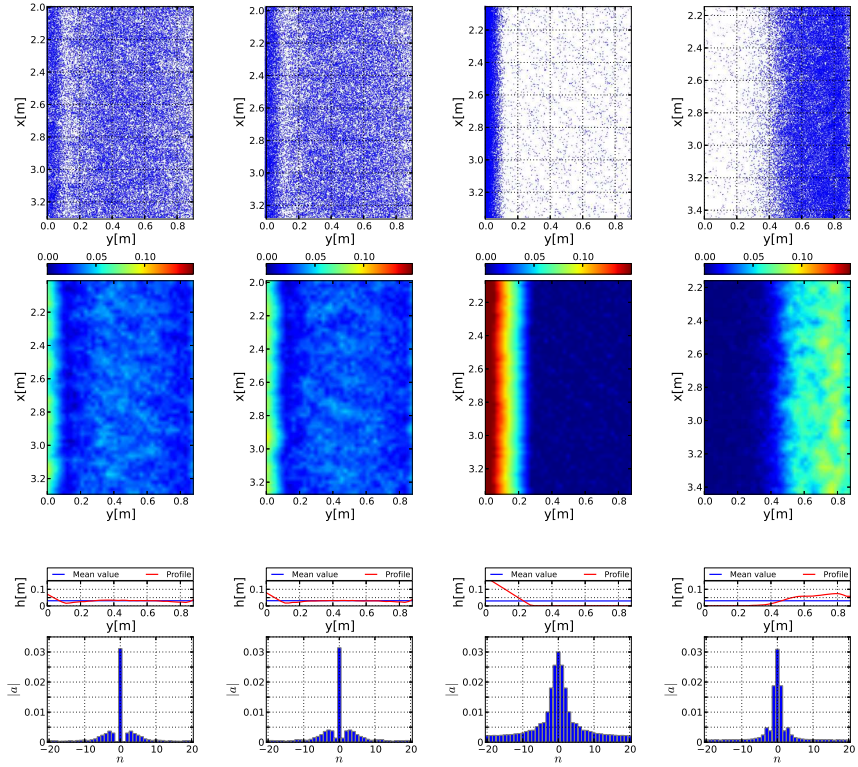


Fig. 9: Simulation sample data from the points I-IV (left to right) in the design space, as described in Table 1. The subplots show raw particle scatter data on the belt conveyor from one drum evolution (first row), reconstructed height surface (second row) with the color indicating the height in units m, time-averaged height profile (third row) and the corresponding FFT spectrum  $\frac{1}{N}||a_n||$  (fourth row).